Received: 24 March 2020 | Revised: 16 July 2020 | Accepted: 30 July 2020

DOI: 10.1111/all.14581

ORIGINAL ARTICLE

Basic and Translational Allergy Immunology

Allergy EUROPEAN JOURNAL OF ALLERGY AND CLINICAL IMMUNOLOGY EAACI WILEY

# Vitamin A controls the allergic response through T follicular helper cell as well as plasmablast differentiation

Josephine Scholz[1,2] | Julia Kuhrau[2,3] | Frederik Heinrich[2] | Gitta Anne Heinz[2] | Andreas Hutloff[2,3,4] | Margitta Worm[1] | Guido Heine[1,2,5]

[1]Division of Allergy and Immunology, Department of Dermatology, Venereology and Allergy, Charité – Universitätsmedizin Berlin, Freie Universität Berlin, Humboldt-Universität zu Berlin, Berlin Institute of Health, Berlin, Germany

[2]Deutsches Rheuma-Forschungszentrum, A Leibniz Institute, Berlin, Germany

[3]Institute of Immunology, University Hospital Schleswig-Holstein, Campus Kiel, Kiel, Germany

[4]Institute of Clinical Molecular Biology, University Hospital Schleswig-Holstein, Campus Kiel, Kiel, Germany

[5]Department of Dermatology and Allergy, University Hospital Schleswig-Holstein, Campus Kiel, Kiel, Germany

**Correspondence**
Guido Heine, Department of Dermatology and Allergy, University Hospital Schleswig-Holstein Campus Kiel, Arnold-Heller-Straße 3, D-24105 Kiel, Germany.
Email: gheine@dermatology.uni-kiel.de

Margitta Worm, Division of Allergy and Immunology, Department of Dermatology, Venereology and Allergy, Charité – Universitätsmedizin Berlin, Charitéplatz 1, D-10117 Berlin, Germany.
Email: margitta.worm@charite.de

**Funding information**
Deutsche Forschungsgemeinschaft, Grant/Award Number: TRR130-P19 and TRR130-P23

## Abstract

**Background:** Vitamin A regulates the adaptive immune response and a modulatory impact on type I allergy is discussed. The cellular mechanisms are largely unknown.

**Objective:** To determine the vitamin A-responding specific lymphocyte reaction in vivo.

**Methods:** Antigen-specific B and T lymphocytes were analyzed in an adoptive transfer airway inflammation mouse model in response to 9-cis retinoic acid (9cRA) and after lymphocyte-specific genetic targeting of the receptor RARα. Flow cytometry, quantitative PCR, next-generation sequencing, and specific Ig-ELISA were used to characterize the cells functionally.

**Results:** Systemic 9cRA profoundly enhanced the specific IgA-secreting B-cell frequencies in the lung tissue and serum IgA while reducing serum IgE concentrations. RARα overexpression in antigen-specific B cells promoted differentiation into plasmablasts at the expense of germinal center B cells. In antigen-specific T cells, RARα strongly promoted the differentiation of T follicular helper cells followed by an enhanced germinal center response.

**Conclusions:** 9cRA signaling via RARα impacts the allergen-specific immunoglobulin response directly by the differentiation of B cells and indirectly by promoting T follicular helper cells.

KEYWORDS

9-cis retinoic acid, allergy, RAR, Tfh cells, vitamin A

**Abbreviations:** 9cRA, 9-cis retinoic acid; ATRA, all-trans retinoic acid; DEG, differentially expressed gene; FDC, follicular dendritic cell; GC, germinal center; GSEA, Gene set enrichment analysis; LPS, Lipopolysaccharide; MFI, mean fluorescence intensity; MSA, Mouse serum albumin; NP, Nitrophenol; padj, adjusted P-value; PMA, Phorbol 12-myritate 13 acetate; RA, retinoic acid; RALDH, retinal aldehyde dehydrogenases; RAR, Retinoic acid receptor; RXR, Retinoid X receptor; Tfh, T follicular helper.

Andreas Hutloff, Margitta Worm, Guido Heine contributed equally to this work.

This is an open access article under the terms of the Creative Commons Attribution-NonCommercial-NoDerivs License, which permits use and distribution in any medium, provided the original work is properly cited, the use is non-commercial and no modifications or adaptations are made.
© 2020 The Authors. *Allergy* published by European Academy of Allergy and Clinical Immunology and John Wiley & Sons Ltd

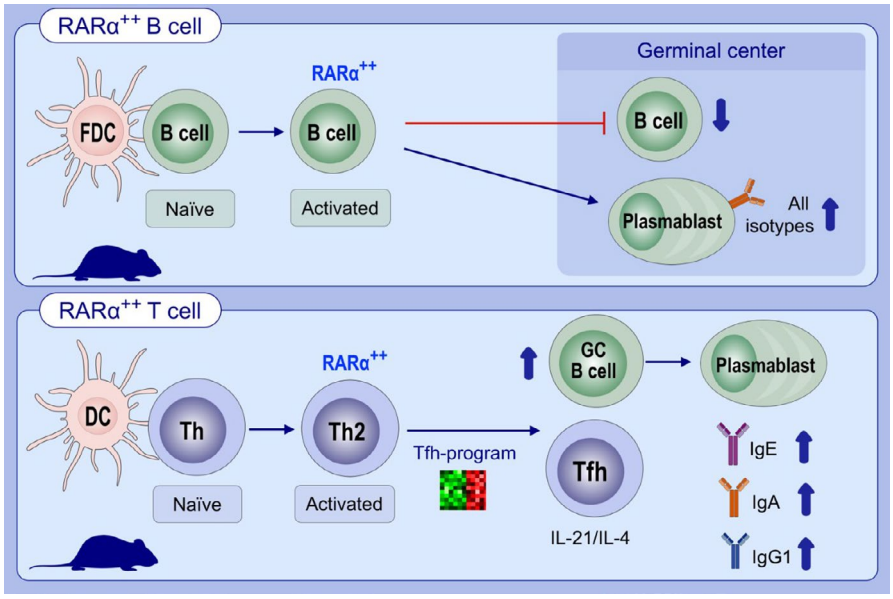


**GRAPHICAL ABSTRACT**

This study analyzes antigen-specific B and T lymphocytes in an adoptive transfer airway inflammation mouse model in response to 9-cis retinoic acid (9cRA) and after lymphocyte-specific genetic targeting of the receptor RARα. RARα overexpression in antigen-specific B cells promotes differentiation into plasmablasts at the expense of germinal center B cells. In antigen-specific T cells, RARα strongly promotes the differentiation of T follicular helper cells followed by an enhanced germinal center response.

## 1 | INTRODUCTION

Type I allergy results from a complex interaction of different immune cell types that promote a B-cell differentiation into IgE secreting cells. In this process, antigen-dependent B-cell activation and differentiation typically take place during the germinal center (GC) reaction in secondary lymphoid organs where the subset of T follicular helper (Tfh) cells provide help via the production of CD40L and IL-21.[1,2] This T-cell subset is characterized by high expression of the transcription factor Bcl-6, Programmed Cell Death Protein (PD)-1, and the chemokine receptor CXCR5 which enables them to migrate into B-cell zones. In this context, vitamin A was recognized as an antigen-independent modulator of the specific humoral immune response.[3-5] The vitamin A deficiency-caused impaired humoral immune response is associated with increased mortality from infections.[6-8] Thus, the WHO recommends vitamin A administration before vaccination against measles, tetanus, or polio in high-risk regions, especially Africa and southern Asia.[9,10] Vitamin A acts through the active metabolite retinoic acid (RA) on lymphocyte activation, proliferation, homing, and through signaling of the nuclear retinoic acid receptors (RARs).[11] These ligand-activated transcription factors dimerize with retinoic X receptors (RXRs) and bind to specific promoter regions. RA is produced by dendritic cells, macrophages, and stromal cells via retinal aldehyde dehydrogenases (RALDH1 and 2) and metabolized through the enzyme CYP26A, which is induced by RA itself.[12] These receptors are widely expressed on different immune cells including T and B lymphocytes and dendritic cells. The functions of RA include the induction of gut-homing molecules such as α4ß7 integrin and CCR9 on lymphocytes.[13,14] The reports on RA functions on T helper cell differentiation and polarization are heterogeneous, suggesting a context-dependent setting.[15-19] While B cells are promoted by RA to differentiate into antibody-secreting cells,[5,20,21] vitamin A deficiency in mice leads to reduced serum IgA and IgG.[22,23] In an established type I allergy model, we identified the physiologic vitamin A metabolite 9-cis retinoic acid (9cRA) as a potent modulator to induce specific IgA response at the expense of IgE in vivo.[24] These observations corroborate data from human B-cell cultures[24,25] and regarding IgE also data from patients during systemic 9cRA-therapy (ie, Alitretinoin).[26] Until now, the cellular mechanism of 9cRA is not known, whether lymphocyte-intrinsic mechanisms or complex interactions between several different cell types including stromal cells are involved. In this work, we investigated the functions of 9cRA, which is used in humans with a beneficial safety profile and previously shown immunomodulatory properties, and followed the hypothesis that RARα functions modulate the differentiation in a lymphocyte-specific manner, that is, the differentiation of B cells into antibody-secreting cells and the polarization of T (follicular) helper cells.

## 2 | MATERIALS AND METHODS

### 2.1 | Mice

All experiments were approved by the local authority (Landesamt für Gesundheit und Soziales, Berlin, Germany) and performed in

accordance with the German animal protection laws. Mice were bred under specific pathogen-free conditions in the DRFZ animal facility at the Federal Institute for Risk Assessment, Berlin. C57BL/6NCrl and CD28 knock-out mice[27] were used as recipients for adoptive transfer. Smarta TCR-transgenic mice[28] were additionally backcrossed to B6PL mice (Jax stock 000406; Thy-1.1$^+$) to track cells after adoptive transfer. For analysis of antigen-specific B cells, nitrophenol (NP)-specific BCR knock-in B1-8i mice[29] were crossed to κ-L chain knock-out mice[30] to ensure NP specificity of all B cells and Ly-5.1 mice (Jax stock 002014; CD45.1$^+$) to track cells via this congenic markers after the transfer (either B220$^-$CD4$^+$ Thy-1.1$^+$ for Smarta-specific T cells or CD4$^-$CD8$^-$CD19$^+$CD45.2$^-$CD45.1$^+$ for NP-specific B cells) (Figure S1). For all experiments, female mice were used at an age of 8-16 weeks.

## 2.2 | Retroviral knockdown and overexpression of T and B cells

For specific RNA interference of RARα, RARα target sequences (5′-TGCAGTTCCGAAGAGATAGTTTCAAGAGAACTATCTCTTCGGAACTGCTTTTTTC-3′) were annealed and DNA oligonucleotides were cloned into the retrovirus-based vector pQCXIX (Takara Bio) containing the murine U6 promoter downstream of an EF1α promotor and GFP fluorescent reporter (described in[31]) using *Hpa*I and *Sal*I restriction sites (Figure S2). As a control, a scrambled sequence (5′-TGCTATCGAGAAGATCAGCCTTCAAGAGAGGCTGATCTTCTCGATAGCTTTTTTC-3′) was used. For constitutive overexpression, cDNA for RARα was amplified from murine spleen using the following primers: RARα forward 5′-GGAAGATCTCCATCACAACTACCTGCC-3′ and RARα reverse 5′ GGACTCGAGGAAGGCAGAGAAAGCCAG-3′ and cloned into the retroviral expression vector pMSCV (Takara Bio) using *Bgl*II and *Xho*I restriction enzymes, followed by an IRES site and mAmetrine as a fluorescent reporter for positive selection (Figure S2).

Viral particles were produced using HEK293T cells transfected with packaging plasmids pECO and pCGP and respective plasmids by calcium phosphate transfection. Retroviral supernatants were collected after 24 and 48 hours.

Splenocytes from Smarta mice were cultured with the addition of LCMV $GP_{61-80}$ peptide (1 μg/mL; GenScript), recombinant IL-4 (10 ng/mL; Miltenyi Biotec), anti-IFN-γ (AN18.17.24; 10 μg/mL), and anti-IL-12 (C17.8; 5 μg/mL) for Th2 polarization (this results in an enhanced frequency of IL-4 producers but not a strict Th2 phenotype, ie, T cells are still able to produce IFN-γ in vivo). After 24 hours of in vitro stimulation, T cells were retrovirally infected as described before.[32] Cells were cultured for an additional 4 days, followed by sorting for cells expressing the corresponding fluorescent protein on a FACSAria II (BD Biosciences) or SH800S Cell Sorter (Sony).

Respectively, splenic B cells from B1-8i mice were sorted magnetically (Miltenyi Biotec) by depletion of CD43 positive cells and stimulated in the presence of NP-Ficoll (Biosearch Technologies, 1 μg/mL) and anti-CD40 (FGK45; 10 μg/mL) for 24 hours before retroviral transduction. 48 hours post-infection, B cells were sorted for positive mAmetrine fluorescence expression.

## 2.3 | Adoptive transfer airway inflammation model and subcutaneous immunization

$2.5 \times 10^5$ Th2-biased Smarta cells were cotransferred with $1 \times 10^6$ retrovirally transduced transgenic B1-8i B cells into C57BL/6 mice by intravenous injection. Alternatively, $2.5 \times 10^5$ retrovirally transduced Smarta cells were cotransferred with $1 \times 10^6$ naive B1-8i B cells into CD28 knock-out mice, which cannot mount an endogenous T-cell response and therefore are ideal to study indirect effects of the modified Smarta T cells on the B-cell response. Before transfer, cells were counted with a Guava EasyCyte capillary flow cytometer and ViaCount solution (Merck Millipore) or sorted via fluorescence-activated cell sorting for GFP or mAmetrine expression. For subcutaneous immunization, recipient mice were injected s.c. at the tail base with 20 μg of a synthetic cognate antigen (LCMV $GP_{61-80}$ peptide and iodo-NP (NIP) conjugated to mouse serum albumin; NIP-SM-MSA) in complete Freund's adjuvant (Sigma-Aldrich) at the tail base.

For induction of airway inflammation, mice were repetitively challenged intranasally with 20 μg NIP-SM-MSA with 5 μg LPS (Sigma-Aldrich) as adjuvant on day 0, 1, 10, and 13. In some experiments, 0.36 mg 9-cis retinoic acid (Enzo Life Science) was given in weekly intervals subcutaneously as described before,[24] starting 2 weeks before adoptive transfer.

## 2.4 | Cell isolation

After subcutaneous immunization, the draining inguinal lymph nodes were isolated on day 7. In the airway inflammation model, the lungs were analyzed on day 7 or 17. After perfusion of the lung with PBS, bronchial lymph nodes were dissected from the lung tissue under a microscope. Single-cell suspensions from lung tissue were prepared using the gentle MACS dissociator (Miltenyi Biotec) and digested with 0.5 mg/mL collagenase D and 20 mg/mL DNase I (both from Roche) for 25 minutes at 37°C. All cells were counted using a Guava EasyCyte capillary flow cytometer and ViaCount solution (Merck Millipore).

## 2.5 | Flow cytometry

Single-cell suspensions from lymph nodes, lung, or cultured Smarta T cells were stained with different combinations of fluorophore-conjugated antibodies (Table S1). Up to $7.5 \times 10^7$ cells resuspended in a total volume of 200 μL in 96 well microplates (round type) were stained. To avoid unspecific antibody binding, cells were first incubated with Fcγ receptor block (2.4G2;

anti-CD16/32). To determine the optimal staining quality of antibodies, the intensity of staining was tested with several dilutions before the experiment. Mix of antibodies diluted in PBS supplemented with 0.25% BSA and 0.1% $NaN_3$ was added to the cells for 30-45 minutes on ice. Staining with biotinylated antibodies required an additional step with fluorophore-labeled streptavidin for 5 minutes. Streptavidin -PE-Cy7, -APC-Cy7, or -PerCP (all from Biolegend) was used as secondary reagents. Dead cells were stained and excluded either by DAPI or propidium iodide, added immediately before analysis.

For intracellular staining of immunoglobulins (also stains surface Ig), transcription factors, or cytokines, cells were fixed and permeabilized after surface staining. Cytokine expression was analyzed after restimulation with phorbol 12-myristate 13-acetate (PMA; 10 ng/mL) and ionomycin (1 μg/mL) for 4 hours at 37°C including 3 hours Brefeldin A (5 μg/mL, Biomol). Prior to fixation, cells were labeled with 84 nmol/L Alexa Fluor-700, Cy7, or Brilliant UV350 succinimidyl ester or 1.34 μmol/L Pacific Orange succinimidyl ester (Invitrogen) on ice for 25 minutes, to discriminate dead cells.[33] For immunoglobulins and cytokines, cells were fixed with 4% paraformaldehyde for 20 minutes at RT, permeabilized by washing and incubating with saponin buffer and stained with different fluorophore-conjugated antibodies (Table S1). Differently, transcription factors (Table S1) were stained using the FoxP3 Staining Buffer Set (eBioscience) and fixed for at least 1 hour at 4°C. Analogous to surface staining, non-specific binding of the antibodies was prevented by pre-incubation of the cells in 20 μg/mL 2.4G2 (anti-CD16/32) for 5 minutes. The staining of intracellular proteins was performed for 30 minutes on ice. For detection of IL-21, an IL-21R-Fc chimera (Table S1), followed by Alexa Fluor 647-conjugated goat anti-human Ig (Jackson ImmunoResearch), was used. Cells were washed before analysis, resuspended in PBS/0.25% BSA/0.1% $NaN_3$, and passed through 70 μm filter fabric. Flow cytometry was performed on an LSR Fortessa or Symphony (BD Biosciences) and data analyzed with FlowJo software (Tree Star). Analysis gates were set on live cells, identified by the exclusion of DAPI-, PI- or fixable live/dead stain-positive cells and defined by scatter characteristics and exclusion of doublets. In all figures, antigen-specific T cells were identified as $B220^-$ $CD4^+$ $Thy\text{-}1.1^+$; antigen-specific B cells as live $CD4^-$ $CD8^-$ $CD19^+$ $CD45.2^-$ $CD45.1^+$.

## 2.6 | Enzyme-linked immunosorbent assay

NP-specific Ig was determined by ELISA as described in.[34] Briefly, after coating of 96-well flat-bottom plates (Nunc MaxiSorp) with NP-coupled BSA (5 μg/mL), followed by incubation with diluted serum, mouse IgG1 or IgA was detected using horseradish peroxidase-coupled monoclonal antibodies (Southern Biotechnologies). NP-specific IgE was determined on plates coated with anti-mouse IgE (clone R35-27; BD Biosciences) and incubation with diluted serum followed by NP-conjugated BSA and biotinylated anti-NP (clone 18.1.16) and peroxidase-conjugated streptavidin. As standard served purified IgA (233.1.3), IgG1 (18.1.16), or recombinant NP-specific antibody (B1-8-IgE, all kindly provided by Klaus Rajewsky). The colorimetric reaction was analyzed for absorbance at 450 nm using a SpectraMax Photometer (Molecular Devices).

## 2.7 | RNA isolation and quantitative PCR

RNA was isolated from sorted lymphocytes using the Direct-zol RNA Kit (Zymo Research) according to the manufacturer's protocol. RNA was reverse transcribed using the High-Capacity cDNA Reverse Transcription Kit (Applied Biosystems). Gene expression was analyzed on a QuantStudio 7 Flex Real-Time PCR System (Applied Biosystems) using TaqMan gene expression assays (Thermo Fisher Scientific) for murine RARα (Mm01296312_m1), Cyp26A1 (Mm00487244_m1), and Hprt for standardization (Mm01545399_m1).

## 2.8 | Next-generation sequencing

RNA samples were purified using the RNeasy Micro Kit (Qiagen) and the quality validated using a Fragment Analyzer System and the HS RNA 15 nt Kit (Agilent Technologies). RNA was classified as suitable if samples showed optimal S28/S18 ratio (≥2.0), displayed no RNA degradation, and had an RNA quality number (RQN) above 8. For gene expression library preparation, 10 ng of total RNA was used as input in the Smart-Seq v4 mRNA Ultra Low Input RNA Kit (Clontech) and processed according to the manufacturer's instructions. After quality control (HS NGS Fragment Kit (1-6000 bp), Agilent) and concentration measurement (Qubit dsDNA HS Assay Kit, Invitrogen), 1 ng of the purified cDNA was used for library completion with the Nextera XT library preparation kit (Illumina). Paired-end sequencing (2 × 75 nt) was performed on an Illumina NextSeq500, and raw sequence reads were mapped to the mouse GRCm38/mm10 genome with TopHat2[35] in very-sensitive settings for Bowtie2.[36] Gene expression was quantified either by HTSeq[37] for total RNA or feature Counts[38] for mRNA and analyzed using DESeq2.[39] Differential expression between empty control vector and RARα overexpression was regarded as significant when the adjusted *P*-value was <0.05 and the log2 fold-change was >1.2.

## 2.9 | Statistical analysis

The sample size was predetermined using G*Power 3.[40] Data are either displayed showing the mean value and results from single animals or the mean with error bars (SEM) as indicated. Data were statistically analyzed using Prism 8 software (GraphPad Software). No data were excluded. Normal distribution was analyzed using the Shapiro-Wilk test, and differences between the groups were evaluated using a two-tailed Student's *t* test or Mann-Whitney *U* test, accordingly.

## 3 | RESULTS

### 3.1 | 9cRA promotes the specific IgA response at the expense of IgE

To elucidate the role of 9cRA on antigen-specific T and B cells in the context of an allergic inflammation in vivo, we applied our established airway allergy transfer model.[34] TCR-transgenic T cells from Smarta mice, which had been cultured in vitro for 5 days under Th2 polarizing conditions to enhance the frequency of IL-4 producing T cells, and naive B cells from B1-8i mice, with a specific receptor for nitrophenol (NP), were adoptively transferred into C57BL/6 recipients (Figure 1A). Mice were repeatedly challenged intranasally with cognate antigen resulting in an allergic lung inflammation with infiltrates of antigen-specific T and B cells. The transferred T and B cells were identified by the respective congenic markers Thy-1.1 and CD45.1 via flow cytometry (in the following termed Smarta-specific T or NP-specific B cells). The model allows to detect classical Tfh, GC B cells and plasmablasts in the lung-draining lymph node as well as Tfh-like and GC-like B cells, which interact in the non-lymphoid inflamed lung tissue, resulting in the local generation of plasmablasts in the lung.[34,41]

The mice received 9cRA subcutaneously in weekly intervals before and after adoptive transfer (Figure 1A). The data show the induction of GC-like B cells in lung tissue characterized by a $CD38^{low}$ $GL7^{high}$ phenotype (Figure 1B). Additional 9cRA decreased the frequency of this cell population ($P < .01$, Figure 1B) and increased those of specific plasmablasts by 1.5 fold ($P < .01$, $CD138^{+}CD19^{low}$ population, Figure 1C). Most plasmablasts were of IgA or IgG1 isotypes in this model (Figure 1D/E). Additional 9cRA increased both the frequencies of IgA-secreting plasmablasts by 2.5 fold compared to control ($P < .0001$, Figure 1E) and the specific serum IgA concentrations ($P < .01$, Figure 1F). Conversely, 9cRA decreased the frequencies of specific IgE secreting plasmablasts and the specific

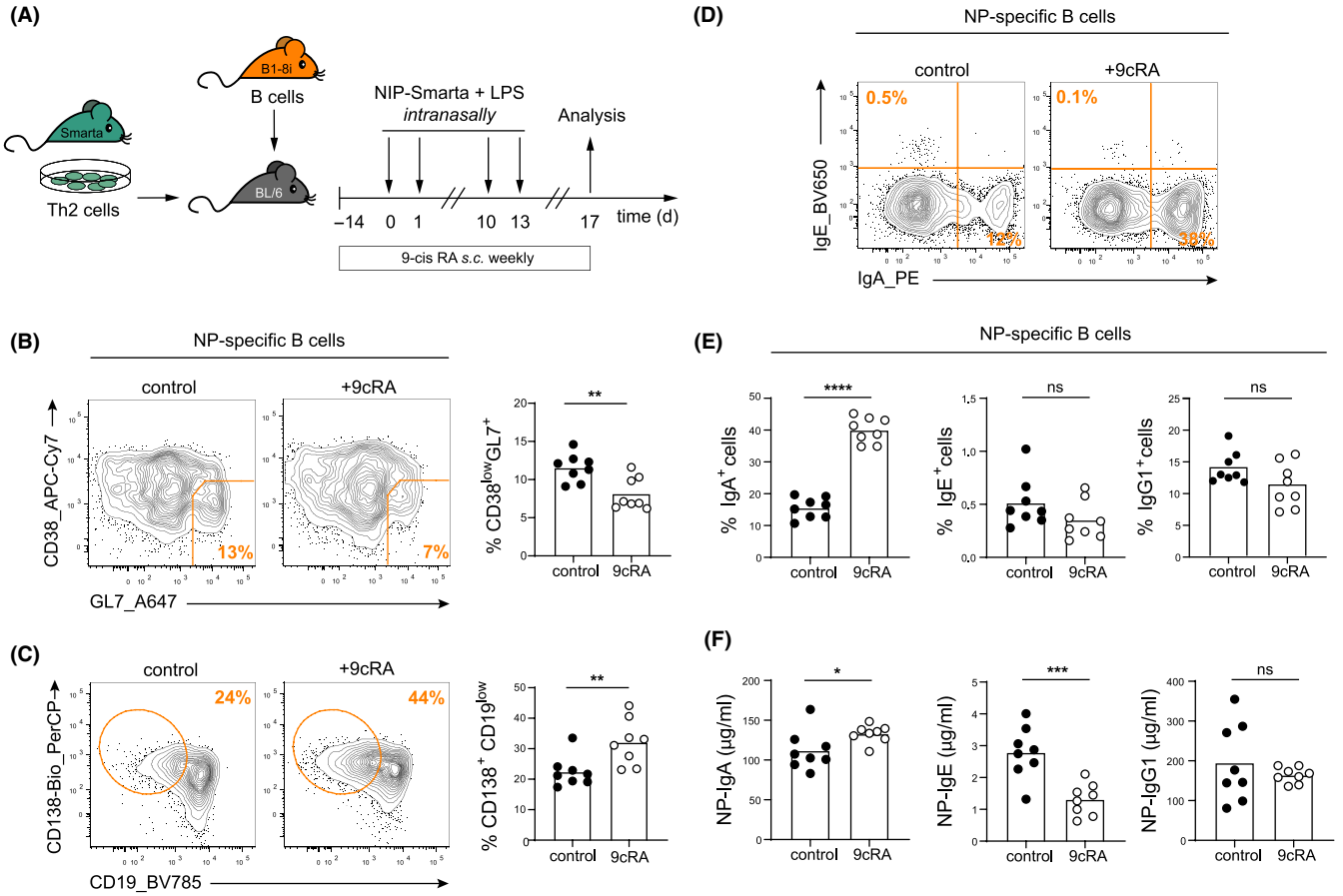


**FIGURE 1** 9cRA promotes the specific IgA response to the expense of IgE. (A) Experimental setup for airway inflammation model. In vitro cultured Smarta-Th2 cells and naive B1-8i B cells were transferred into syngeneic C57BL/6 mice, some of which treated with 9cRA weekly. After repeated cognate antigen challenge, antigen-specific T and B cells were analyzed from lung as indicated. (B) Quantification of $CD38^{low}GL7^{+}$ GC-like B cells in lung tissue. The flow cytometry contour plots are gated on NP-specific B cells and the frequencies are shown in % of the NP-specific B cells. (C) Analysis of NP-specific $CD138^{+}CD19^{low}$ plasmablasts was performed accordingly and representative contour plots and statistic evaluation is shown. (D) Representative flow cytometric staining of NP-specific B cells in the lung regarding the isotype class. (E) Statistical analysis of the immunoglobulin-secreting NP-specific B cells from lung tissue. (F) Serum concentrations of antigen-specific IgA, IgE, and IgG1 as determined by ELISA. Each symbol represents a single animal and bars depict the mean. Data are representative of two independent experiments with 4 animals per group and per experiment. Two-tailed Student's *t* test for normally distributed data (Shapiro-Wilk normality test): $^{*}P < .05$; $^{**}P < .01$; $^{***}P < .001$; $^{****}P < .0001$; ns $P > .05$

IgE serum concentrations ($P < .001$, Figure 1E/F). Frequencies of NP-specific IgG1 plasmablasts and serum concentrations were comparable between both groups ($P > .05$, Figure 1E/F), suggesting an isotype-specific effect of 9cRA on IgA and IgE.

Thus, we show that 9cRA promotes a specific IgA response to the expense of IgE in our antigen-specific transfer model and determines the immune reaction in both, the lymphatic tissue and the inflamed lung tissue.

### 3.2 | RARα promotes B-cell differentiation into plasmablasts, but not germinal center B cells

To further investigate the mechanism of how 9cRA controls the specific IgA and IgE response at the cellular level, we ectopically overexpressed its receptor RARα in B cells before transfer. Splenic naive B cells from B1-8i mice were stimulated with NP-Ficoll plus anti-CD40 and transduced with a retroviral vector containing RARα cDNA followed by an IRES site and mAmetrine as a fluorescent reporter protein. The functional overexpression was validated by quantifying the mRNA expression of RARα and the canonical downstream target gene Cyp26A1 ($P < .0001$, Figure 2A). The transduced B cells were adoptively transferred together with Th2-biased SM T cells into recipient mice followed immediately by intranasal antigen challenge (Figure 2B). The recipient mice were kept on a standard diet. Kinetic studies identified day 7 as the optimal time point for the recovery of the activated antigen-specific B cells (data not shown). Transferred activated B cells were able to differentiate into specific GC-like B cells and antibody-secreting cells (Figure 2C/D). Additional RARα overexpression reduced the frequencies of specific GC-like B cells in lung tissue by a factor of two ($P < .001$, Figure 2C). As observed on 9cRA supplementation, the frequencies of CD138$^+$

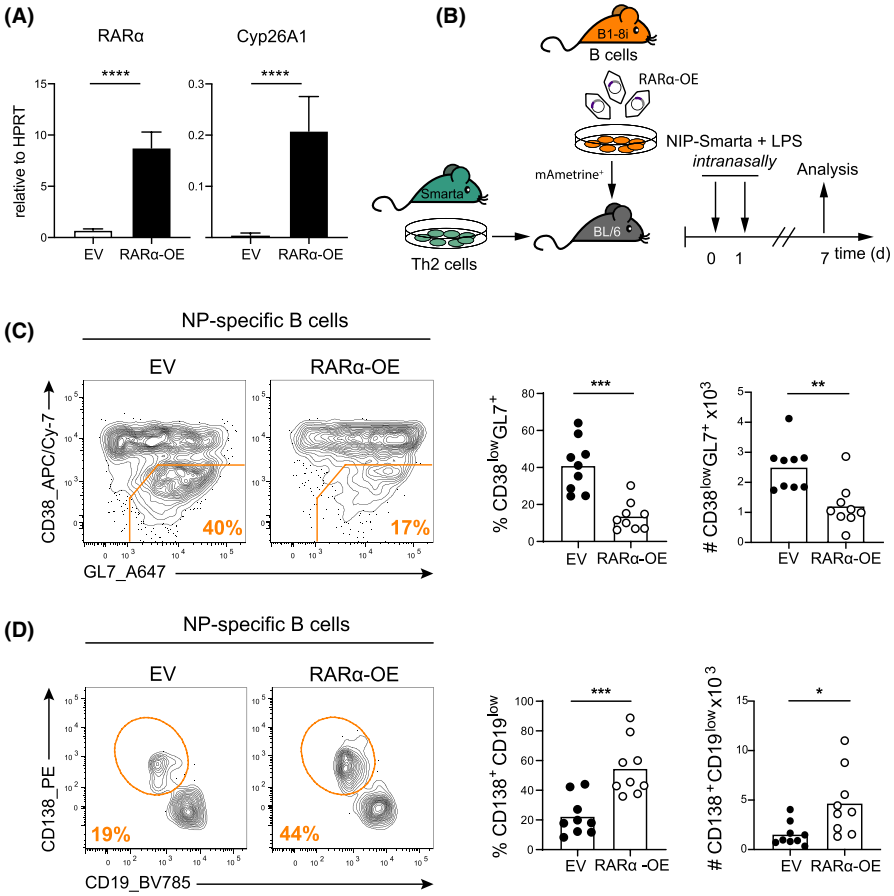


**FIGURE 2** RARα promotes B-cell differentiation into plasmablasts, but not germinal center B cells. (A) Activated B1-8i B cells were retrovirally transduced with RARα overexpression (RARα-OE) or empty control vector (EV), sorted for successfully transduced cells 48-96 h later and analyzed by qPCR for mRNA expression of RARα and Cyp26A1. (B) Experimental setup for airway inflammation model. In vitro activated B1-8i B cells were retrovirally transduced with a RARα overexpression vector or empty vector control and cotransferred with Th2-biased Smarta T cells into syngeneic C57BL/6 mice. On indicated days, recipient mice were immunized with an NIP-Smarta conjugate and LPS intranasally. Antigen-specific B cells from lung were analyzed on day 7. (C) Quantification of CD38$^{low}$GL7$^+$ GC-like B cells in lung tissue. The flow cytometry contour plots are gated on Ag-specific B cells and the frequencies and total numbers are shown of the Ag-specific B cells. (D) Analysis of NP-specific CD138$^+$CD19$^{low}$ plasmablasts was performed accordingly and representative contour plots and statistic evaluation is shown. Each symbol represents a single animal and bars depict the mean. Data are representative of two independent experiments with 4 or 5 animals per group and per experiment. Two-tailed Student's *t* test for normally distributed data or Mann-Whitney test for nonparametric data (Shapiro-Wilk normality test): *$P < .05$; **$P < .01$; ***$P < .001$; ****$P < .0001$

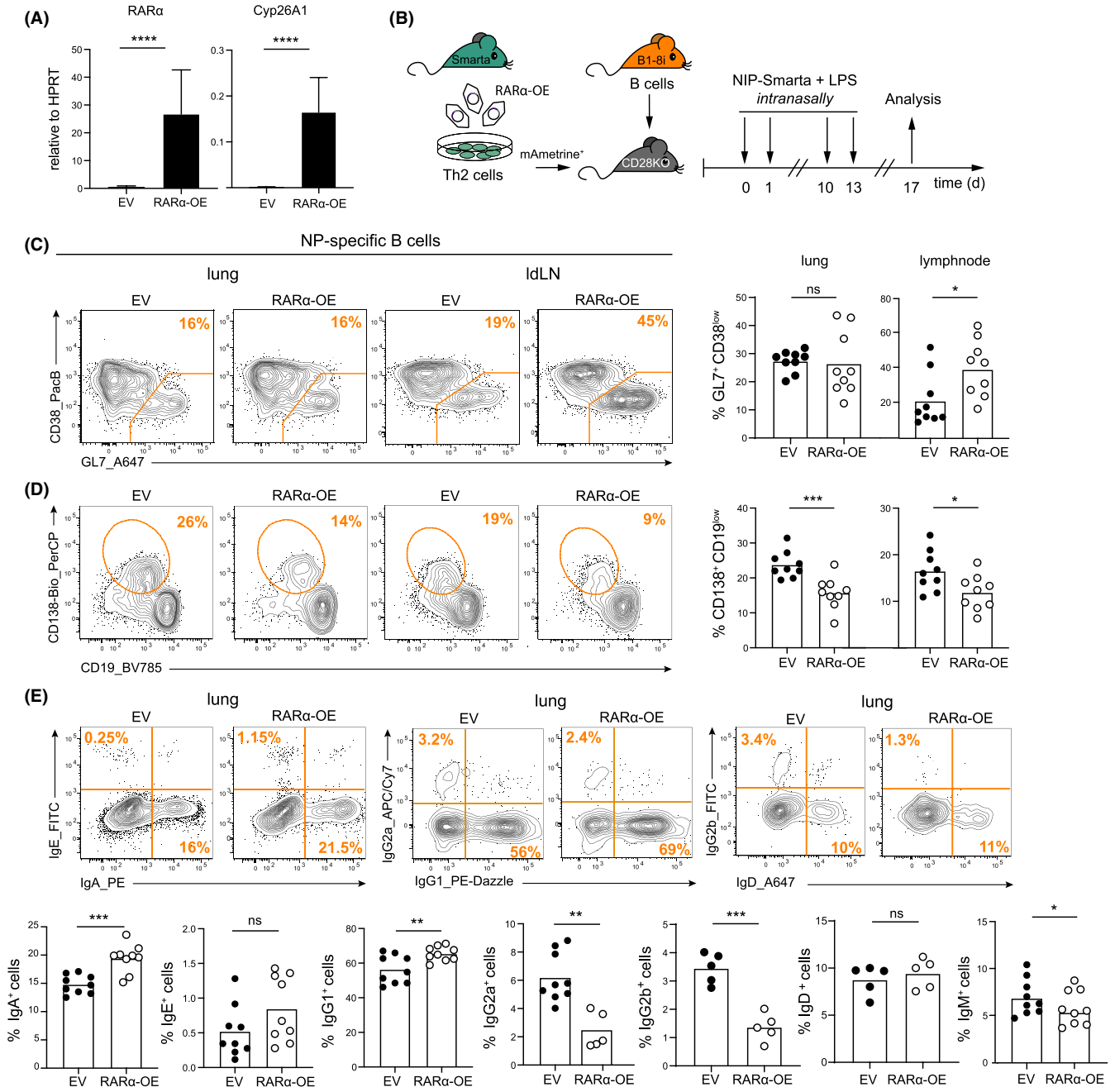


**FIGURE 3** RARα regulates B-cell responses. (A) Activated Smarta T cells were retrovirally transduced with RARα overexpression (RARα-OE) or empty control vector (EV), sorted for successfully transduced cells 48-96 h later and analyzed by qPCR for mRNA expression of RARα and Cyp26A1. (B) Experimental setup for airway inflammation model. Smarta Th2 cells retrovirally transduced with a RARα overexpression vector or empty vector control were adoptively transferred into CD28KO recipients. On indicated days, mice were immunized with an NIP-Smarta conjugate and LPS intranasally. Antigen-specific B and T cells from lung and lung-draining lymph node (IdLN) were analyzed on day 17. (C) Quantification of $CD38^{low}GL7^{+}$ GC-like B cells in lung tissue and $CD38^{low}GL7^{+}$ GC B cells in lung-draining lymph node. The flow cytometry contour plots are gated on Ag-specific B cells and frequencies are shown in % of the NP-specific B cells. (D) Analysis of NP-specific $CD138^{+}CD19^{low}$ plasmablasts was performed accordingly and statistic evaluation is shown. (E) Representative flow cytometric staining of NP-specific B cells in the lung regarding the isotype class and bar graphs showing the frequency of IgA, IgE, IgG1, and IgM secreting B cells (intracellular flow cytometric staining for IgA, IgE, IgG1, IgM) within Ag-specific B cells. Each symbol represents a single animal and bars depict the mean. Data are representative of two independent experiments with 4 or 5 animals per group and per experiment. Two-tailed Student's *t* test for normally distributed data or Mann-Whitney test for nonparametric data (Shapiro-Wilk normality test): $^{*}P < .05$; $^{**}P < .01$; $^{***}P < .001$; $^{****}P < .0001$

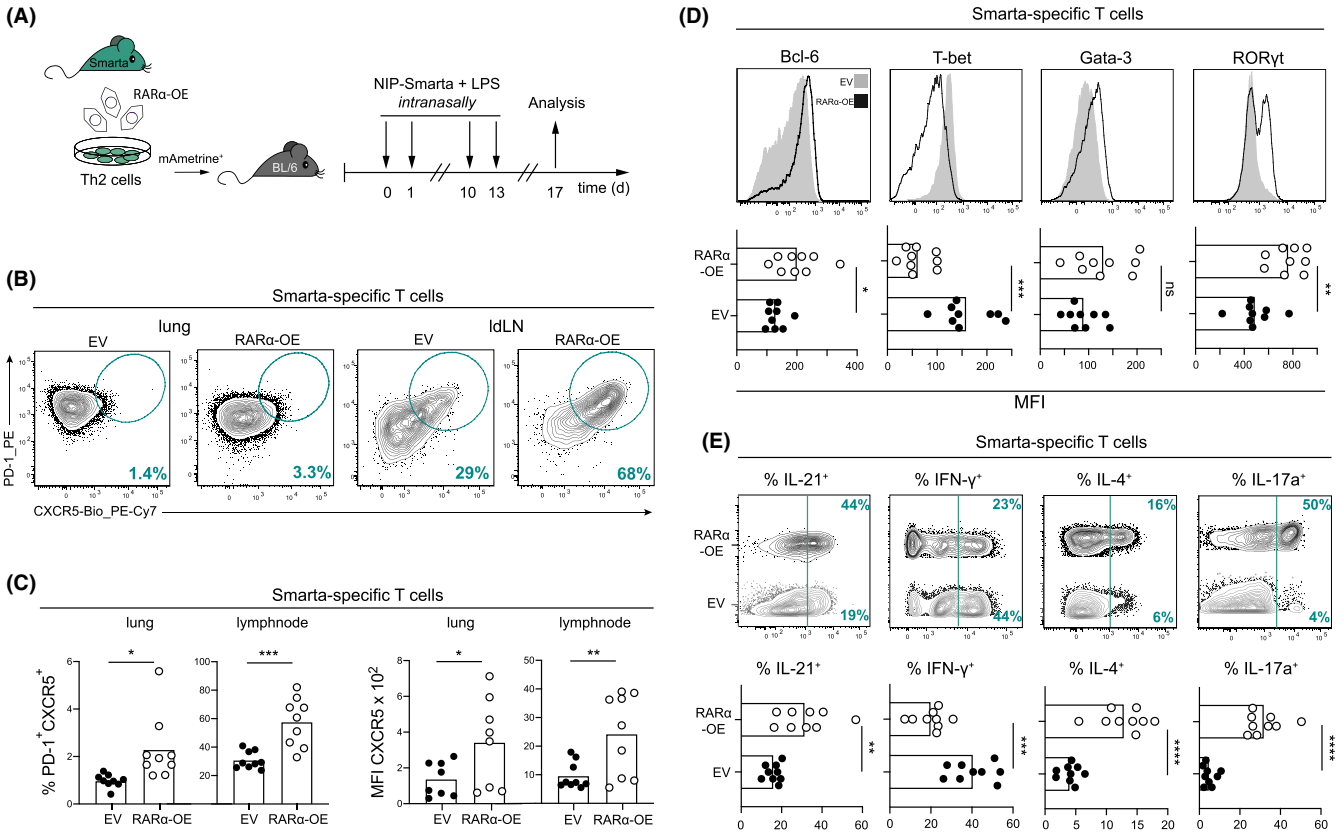


**FIGURE 4** RARα promotes Tfh-cell differentiation. (A) Experimental setup. Smarta Th2 cells retrovirally transduced with a RARα overexpression vector or empty vector control were adoptively transferred into C57BL/6 recipients. On indicated days, mice were immunized with a NIP-Smarta conjugate and LPS intranasally. Antigen-specific T cells from lung and lung-draining lymph node (ldLN) were analyzed on day 17. (B) Representative flow cytometric staining of Smarta-specific T cells in the lung and lung-draining lymph node regarding a PD-1$^+$ CXCR5$^+$ Tfh-cell phenotype, gated on Ag-specific T cells. (C) Statistical analysis of PD-1$^+$ CXCR5$^+$ Tfh cells from lung tissue and lung-draining lymph node. Expression of CXCR5 displayed as bar graph with the geometric mean fluorescence intensity (MFI). (D) Expression of Bcl-6, Gata-3, T-bet, and RORγt by antigen-specific T cells, displayed as representative histograms and bar graphs with the geometric mean fluorescence intensity (MFI). (E) Cytokine expression by antigen-specific T cells. Cells isolated from lung tissue were restimulated in vitro with PMA/ionomycin and cytokine expression was analyzed by flow cytometric intracellular cytokine staining. The flow cytometry contour plots are gated on Ag-specific T cells and frequencies are shown as percentage of Smarta-specific T cells. Dots represent individual mice and bars indicate the mean. Data are representative of two independent experiments with 4 or 5 animals per group and per experiment. Two-tailed Student's *t* test for normally distributed data or Mann-Whitney test for nonparametric data (Shapiro-Wilk normality test): **P* < .05; ***P* < .01; ****P* < .001; *****P* < .0001; ns *P* > .05

CD19$^{low}$ plasmablasts increased 3-fold after overexpression of RARα (*P* < .001, Figure 2D). Analysis of the Ig-isotype in this model showed equal frequencies of specific IgA, IgE, or IgG1 secreting plasmablasts and serum Ig concentrations by genetic modification of RARα in B cells, compared to the control group (Figure S3). Hence, the data show that B-cell-intrinsic RARα-signaling promotes the plasmablast differentiation, but in contrast to 9cRA supplementation does not change the Ig-isotype switch.

## 3.3 | RARα regulates the humoral immune response via T follicular helper cells

Next, we investigated whether 9cRA might control the Ig-isotype via altered T-cell help. Therefore, RARα-overexpressing CD4$^+$ cells were analyzed over time in our adoptive transfer model. Retroviral overexpression in Smarta T cells was effective and functional as the mRNA expression of RARα and the target gene Cyp26A1 was strongly increased compared to the control (*P* < .0001, Figure 3A). To investigate the impact on specific T- and B-cell differentiation, retrovirally transduced cells were transferred together with naïve B cells from B1-8i mice into CD28 knock-out recipient mice. The recipient mice were kept on a standard diet. The lung and the draining lymph nodes were analyzed on day 17 after repeated intranasal immunization (Figure 3B). Overexpression of RARα in T cells increased the frequency of GC B cells in the lung-draining lymph node 2-fold (*P* < .05, Figure 3C), but not the GC-like B cells in lung tissue (*P* > .05, Figure 3C). Conversely, the T-cell-specific overexpression of RARα significantly decreased the frequency of CD138$^+$CD19$^{low}$ plasmablasts in lung-draining lymph node as well as lung tissue (*P* < .001, Figure 3D). As shown in Figure 3E, the overexpression of RARα in specific T cells resulted in increased frequencies of IgA (*P* < .001) and

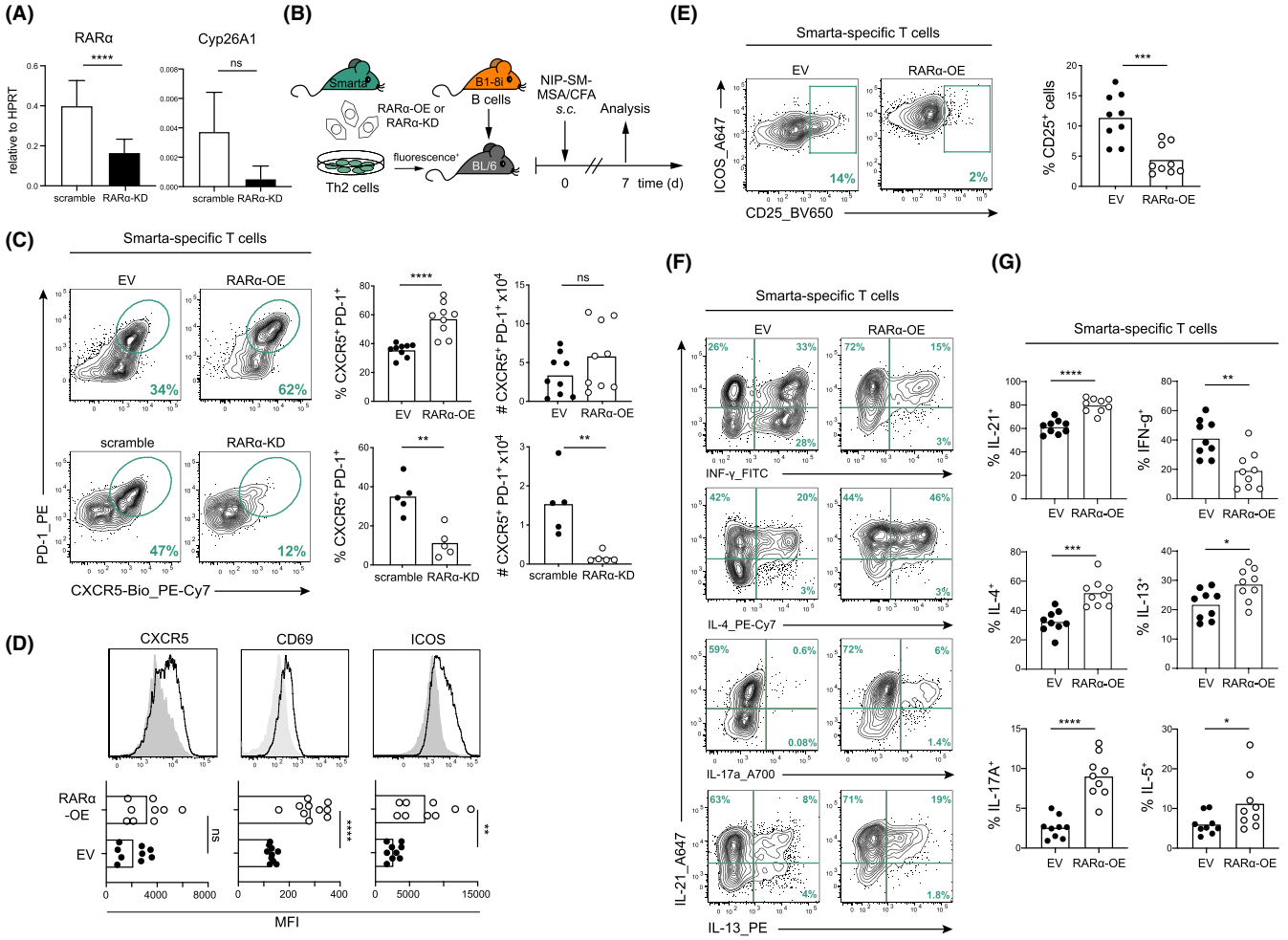


**FIGURE 5** RARα promotes Tfh-cell differentiation and production of B-cell stimulating cytokines. (A) Activated Smarta T cells were retrovirally transduced with an shRNA vector for RARα knockdown (RARα-KD) or a scramble sequence, sorted for successfully transduced cells 48-96 h later and analyzed by qPCR for mRNA expression of RARα and Cyp26A1. Data are shown from three independent experiments. (B) In an independent setup, Smarta T cells were retrovirally transduced with a RARα overexpression (RARα-OE) or shRNA-mediated RARα-knockdown (RARα-KD) and sorted for adoptive transfer into WT recipients. Draining lymph nodes were analyzed 7 days after s.c. immunization for Tfh-cell differentiation, homing and activation molecules and cytokine production. (C) Antigen-specific T cells were analyzed by flow cytometry for a PD-1$^+$CXCR$^+$ Tfh phenotype. (D) Expression of CXCR5, CD69, and ICOS analyzed by flow cytometry and displayed as representative histograms and as bar graph with the geometric mean fluorescence intensity (MFI). (E) Antigen-specific T cells were analyzed by flow cytometry for CD25 expression. (F + G) Cytokine expression by antigen-specific T cells. Cells isolated from inguinal lymph node were restimulated in vitro with PMA/ionomycin and cytokine expression was analyzed by flow cytometric intracellular cytokine staining. Dots represent individual mice and bars indicate the mean. Data are representative of one or two independent experiments with 4 or 5 animals per group and per experiment. Two-tailed Student's *t* test for normally distributed data or Mann-Whitney test for nonparametric data (Shapiro-Wilk normality test): *$P < .05$; **$P < .01$; ***$P < .001$; ****$P < .0001$; ns $P > .05$

IgG1 ($P < .01$) secreting B cells in the lung, with unchanged IgE and IgD ($P > .05$) and decreased IgG2b ($P < .001$), IgG2a ($P < .01$), and IgM secreting B cells ($P < .05$, Figure 3E). Thus, RARα in T cells strongly impacts the differentiation of B cells into antibody-secreting cells.

As IgA and IgG1 are mostly derived from germinal center reactions, we investigated the functional role of RARα on T-cell subset differentiation in a separate experiment where retrovirally transduced RARα-overexpressing Th2-biased Smarta cells were transferred into C57BL/6 recipient mice (Figure 4A), which were kept on a standard diet. The data show that RARα overexpression in antigen-specific T cells strongly promoted the differentiation into Tfh cells characterized by surface co-expression of CXCR5 and PD-1 in the lung and the draining lymph node (Figure 4B/C). We next determined the expression of the master transcription factors and cytokines distinguishing Th1, Th2, and Th17 helper cells. Supporting the upregulation of CXCR5 on T cells with RARα overexpression in the lung, Bcl-6 expression was higher in these cells ($P < .05$, Figure 4D). Similar results were obtained for IL-21, which is the major secreted cytokine of Tfh cells ($P < .01$, Figure 4E). Moreover, RARα overexpression resulted in substantially lower expression of T-bet, stable GATA3, and induced RORγt on a subpopulation of the antigen-specific T cells ($P < .001$, $P > .5$, and $P < .0001$, Figure 4D).

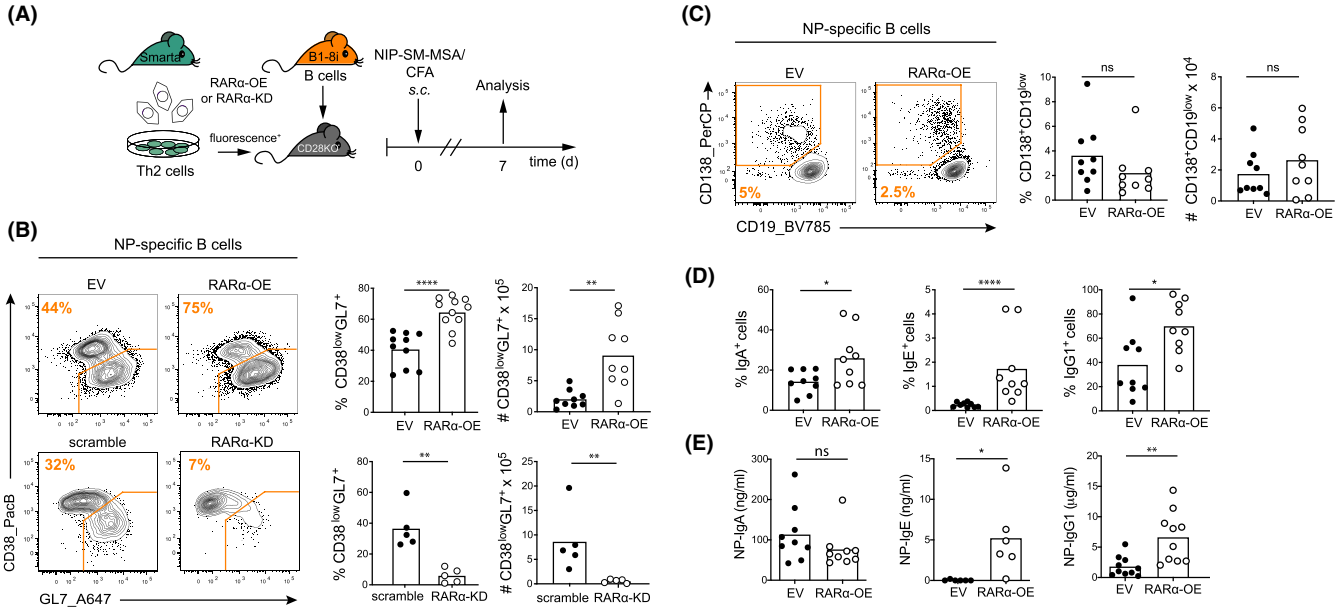


**FIGURE 6** T-cell-specific RARα-overexpression promotes germinal center B-cell formation and triggers the humoral immune response. (A) In two independent setups, Smarta T cells were retrovirally transduced with either a RARα overexpression (RARα-OE) or shRNA-mediated RARα-knockdown (RARα-KD) vector for adoptive transfer into CD28 knock-out recipients. NP-specific B1-8i B cells were cotransferred to analyze the impact on the germinal center reaction. Seven days after *s.c.* immunization, inguinal lymph nodes were analyzed for GC B-cell differentiation and antibody-secreting B cells. (B) Quantification of $CD38^{low}GL7^{+}$ GC B cells. Shown are representative plots and bar graphs with frequencies as percentage of the NP-specific B cells. (C) Analysis of NP-specific $CD138^{+}$ $CD19^{low}$ plasmablasts was performed accordingly and statistic evaluation is shown. (D) Bar graphs showing the frequency of IgA, IgE, and IgG1 secreting B cells (intracellular flow cytometric staining for IgA, IgE, and IgG1) within Ag-specific B cells. (E) Serum concentrations of antigen-specific IgA, IgE, and IgG1 as determined by ELISA. Dots represent individual mice, and bars indicate the mean. Data are representative of one or two independent experiments with 4 or 5 animals per group and per experiment. Two-tailed Student's *t* test for normally distributed data or Mann-Whitney test for nonparametric data (Shapiro-Wilk normality test): $^{*}P < .05$; $^{**}P < .01$; $^{****}P < .0001$; ns $P > .05$

The frequencies of T cells secreting IFN-γ were decreased, but 3-fold increased for IL-4 and IL-17A ($P < .001$, $P < .0001$ and $P < .01$, Figure 4E). Kinetic studies showed that already 7 days after transfer RARα overexpression in T cells increased the frequencies of Tfh and plasmablasts (Figure S4). Taken together, RARα strongly promotes directly and long-lasting the Tfh-cell differentiation in T helper cells in vivo, showing a unique cytokine pattern with increased IL-4 and IL-17A and less IFN-γ.

## 3.4 | RARα-mediated transcriptional program differentiates Tfh2, Tfh13, and Tfh17 cells

To validate whether RARα can regulate Tfh cells in a reciprocal approach, we used an shRNA-mediated knockdown approach, which resulted in reduced mRNA expression of RARα and the target gene Cyp26A1 ($P < .0001$ for RARα, Figure 5A). To characterize the Tfh-cell phenotype following RARα overexpression or knockdown in more detail, we switched to a simpler mouse model with subcutaneous antigen application at the tail base and analysis of the draining inguinal lymph node (Figure 5B), which we had previously used to study Tfh-cell differentiation in vivo.[32,42] After 7 days, Tfh-cell frequencies in the lymph node were increased by RARα overexpression ($P < .0001$) and conversely reduced by RARα-specific shRNA-mediated knockdown ($P < .01$, Figure 5C). The phenotype of RARα overexpressing T cells resembles Tfh cells by high levels of CXCR5 ($P > .05$), the costimulatory molecule ICOS ($P < .01$; a marker of Tfh cells and essential for germinal center formation[42-44]) and CD69 ($P < .0001$; retaining Tfh cells in the lymphoid tissue in local proximity to B-cell follicles[45]; Figure 5D). Moreover, the upregulation of the IL-2 receptor CD25 on a subset of T cells is almost completely blocked by RARα ($P < .0001$, Figure 5E). In line with this finding, it has been shown that IL-2 receptor signaling blocks Tfh-cell differentiation by direct repression of Bcl-6.[46-49] Supporting the specificity of our findings in the allergic airway inflammation model, a functional Tfh-cell phenotype by RARα overexpression was determined by more $IL\text{-}21^{+}$ ($P < .0001$) together with $IL\text{-}4^{+}$ ($P < .001$), $IL\text{-}5^{+}$ ($P < .05$), $IL\text{-}13^{+}$ ($P < .05$) and $IL\text{-}17A^{+}$ ($P < .0001$) and less IFN-$\gamma^{+}$-secreting T cells ($P < .01$) compared to the control group (Figure 5F/G). In linen with these findings, RARα knockdown resulted in reduced $IL\text{-}4^{+}$ ($P < .05$), $IL\text{-}13^{+}$ ($P < .01$), and $IL\text{-}17^{+}$ ($P < .001$)-secreting T cells (Figure S5). The strong correlation of these cytokines with IL-21 expression suggests that retinoic acid signaling promotes the development of Tfh cells of the Tfh2, Tfh13, and Tfh17 subtype.

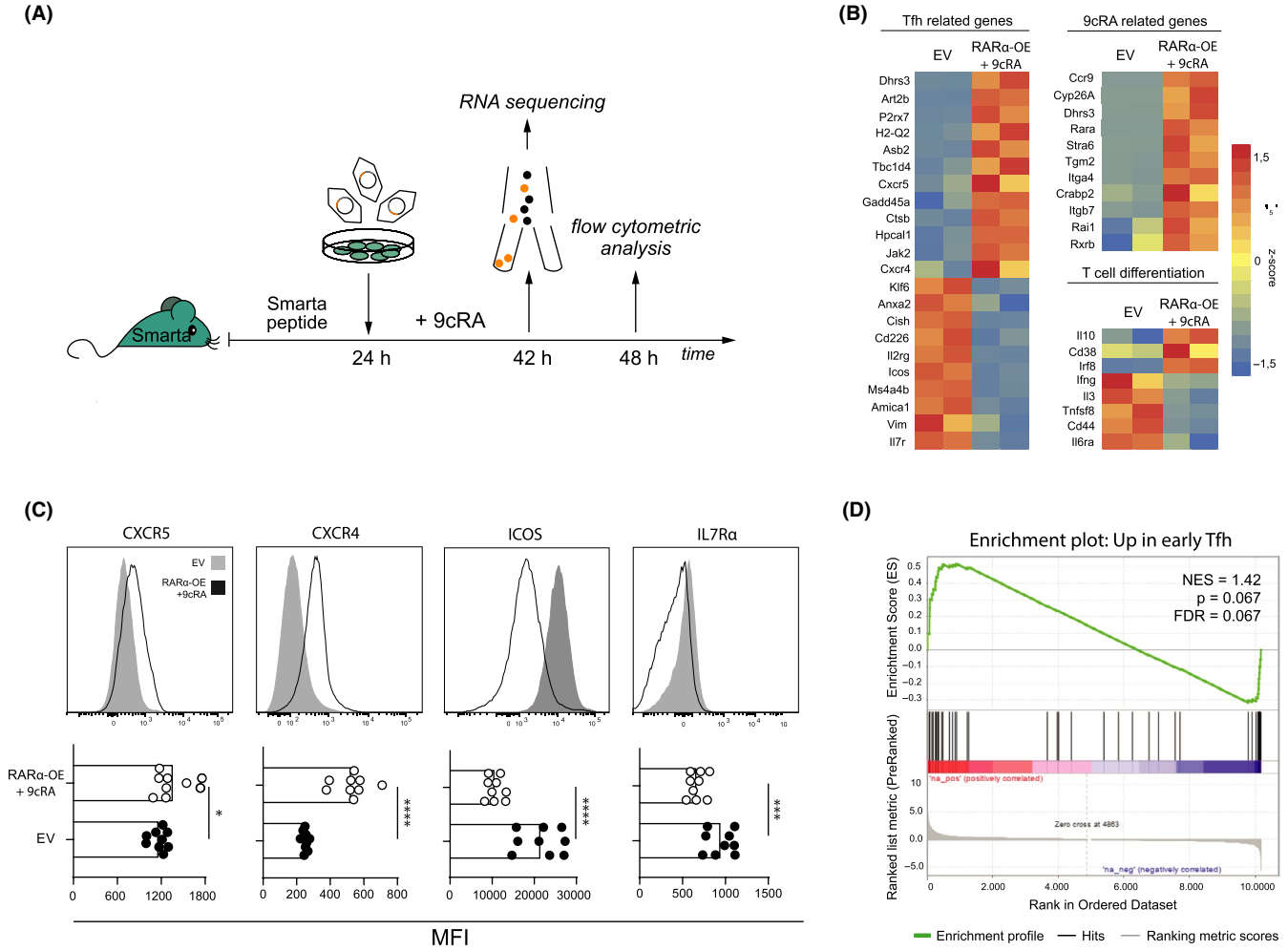


**FIGURE 7** RARα regulates Tfh-cell-associated genes in T helper cells. (A) Smarta T cells were stimulated for 24 h in vitro, retrovirally transduced with RARα overexpression or empty control vector, sorted for successfully transduced cells 18 h later and analyzed by RNA sequencing. (B) Heat maps revealing genes that are differentially expressed in RARα overexpressing cells vs control of two independent experiments. (C) Retrovirally infected Smarta T cells were analyzed by flow cytometry for CXCR5, CXCR4, ICOS, and IL-7R expression 24 h after infection. Data are shown from three independent experiments. *$P < .05$; ***$P < .001$; ****$<P < .0001$. (D) Gene Set Enrichment Analysis of differentially regulated genes showing gene sets upregulated in early Tfh cells relative to genes regulated by RARα-overexpressing T cells

## 3.5 | Increased germinal center and humoral immune response by RARα-induced Tfh cells

To further determine the function of the RARα-induced Tfh cells, naive B cells from B1-8i mice were transferred with T cells after RARα overexpression or knockdown and the germinal center B reaction was determined after 7 days (Figure 6A). The frequency of GC B cells ($CD38^{low}$ $GL7^{+}$) among antigen-specific B cells was increased after the transfer of T cells overexpressing RARα ($P < .0001$), resulting in 3-fold higher total numbers ($P < .01$, Figure 6B). Conversely, shRNA-mediated knockdown of RARα reduced GC B cells by 60% ($P < .01$, Figure 6B). After overexpression of RARα in T cells, the frequency of specific plasmablasts was not altered significantly ($P > .05$, Figure 6C). The proportion of the switched isotype-producing cells was all increased including IgA ($P < .05$), IgE ($P < .0001$), and IgG1 ($P < .05$), which was most pronounced with IgE compared to the empty vector control group (Figure 6D). Accordingly, specific IgE ($P < .05$) and IgG1 ($P < .01$) concentrations were increased in the sera of T-cell-specific RARα-overexpressing mice (Figure 6E). Taken together, RARα-induced Tfh cells promote the germinal center reaction, inducing differentiation of B cells into antibody-secreting cells without priming for a specific Ig-isotype.

## 3.6 | RARα regulates Tfh-cell-associated genes in T helper cells

To understand the mechanism of how RARα induces Tfh-cell differentiation, we performed a global transcriptome analysis by next-generation mRNA sequencing from Smarta T cells 18 hours after RARα-overexpression in the presence of 9cRA in vitro (Figure 7A). 372 genes were found to be differentially expressed (DEG)

between RARα-overexpression and control (>log2 1.2-fold difference and padj < 0.05, Table S2). The most prominent regulated genes were known RARα downstream targets including *Cyp26a1*, *Dhrs3*, *Stra6*, *Tgm2*, *Ccr9*, *Itga4*, and *Itgb7* (Figure 7B). Also, *Il10* and *Cd38* were upregulated in murine RARα-T cells (Figure 7B), as observed previously in activated human B cells in response to 9cRA.[24] The comparison of DEGs in RARα Smarta T cells with a core signature of 304 Tfh-related genes (compiled from two recent publications[32,42]) revealed 45 commonly regulated genes from which the top 22 are shown in Figure 7B. Gene set enrichment analysis (GSEA) confirmed this highly significant enrichment for genes differentially regulated in Tfh cells (Figure S6). The differential regulation of the four most prominently regulated genes *Cxcr5*, *Cxcr4*, *Icos*, and *Il7r* was validated at the protein level by flow cytometry (Figure 7C). Strikingly, ICOS, a gene commonly associated with Tfh cells, was downregulated by RARα overexpression. However, it should be noted that ICOS plays an important role for the maintenance of Tfh cells in late phases of the GC reaction, but has no role in early Tfh-cell differentiation.[42]

To further confirm that RARα overexpression induces a signature of early Tfh-cell development, we sorted Smarta-specific T cells 3 days after transfer and subcutaneous immunization into $CD25^{high}$ effector T cells and $CD25^{neg}$ early Tfh cells (Table S3). Next-generation sequencing identified 70 differentially regulated genes (50 upregulated and 20 downregulated in Tfh vs non-Tfh cells; >log2 1.2-fold difference and padj < 0.05). GSEA using the genes upregulated in early Tfh cells as a gene set shows a strong enrichment of these genes in RARα-overexpressing T cells in the presence of 9cRA (Figure 7D). Taken together, these data identify RARα as an important inducer of Tfh-cell differentiation by regulation of a complex transcriptional mechanism for the first time.

## 4 | DISCUSSION

In this study, we dissected the cell type-specific functions of 9cRA on allergen-specific B and T lymphocytes in vivo. The data obtained from our allergy transfer model decipher direct effects in lymphocytes. RARα signaling in B cells promoted the differentiation into antibody-secreting cells whereas signaling in T cells induced Tfh-cell differentiation and thereby indirectly induced the differentiation of germinal center B cells. These different cell-specific functions of RARα, controlled in our experiments at a genetic level, provide new insight into the complex function of retinoic acid on the humoral immune response in type I allergy.

First, by applying 9cRA to the recipient mice systemically after transferring specific lymphocytes targeting all immune cells during the antigen challenges, we observed enhanced differentiation of plasmablasts secreting specific IgA to the expense of IgE compared to vehicle control and stable IgG1. These data resemble findings from systemic RA treatment of wildtype mice[21] and also from human B cells cultured with 9cRA in vitro.[21,24,25,50,51] Showing that systemic 9cRA efficiently targets the humoral immune response in our model, it is suitable to further investigate lymphocyte-specific functions of RARα by genetic modification before adoptive transfer.

To our knowledge, this is the first report on B-cell-specific after overexpression of RARα in vivo. Our data clearly show an enhanced differentiation into plasmablasts even in the absence of additional exogenous 9cRA, which underlines the long-lasting functionality of the effective overexpression determined at the molecular level in vitro. Also in human B cells, RA was shown to induce plasmablast differentiation,[20,52,53] which suggests an evolutionary conserved mechanism. Our data complement the findings from mice with B-cell-specific absence of RARα signaling, in which plasmablast responses were impaired.[54] However, in contrast to systemic 9cRA, the impact of RARα overexpression on the specific Ig response was isotype independent showing that additional tissue-specific or B-cell-independent mechanisms are required to upregulate IgA and inhibit IgE, indicating the dependence on T-cell help.

Surprisingly, ectopic RARα overexpression in T cells resulted in Tfh-cell induction and pronounced GC reactions. By showing this using two independent routes of antigen delivery, namely airway challenge, and subcutaneous injection, and findings in lymph nodes and the inflamed lung locally, a general RARα-specific mechanism is likely. Our transcriptome studies of RARα-expressing T cells revealed a Tfh-cell gene signature, with dominant upregulation of *Cxcr5* and *Cxcr4*. Indeed, RARα-binding sites have been described in the distal portion of the *Cxcr5* gene.[55,56] These RARα-induced Tfh cells, characterized by expression of Bcl-6, RORγt, IL-21, IL-4, IL-13, and IL-17A but not IFN-γ, promoted differentiation of IgA, IgE, and IgG1 secreting B cells. Our findings are supported by previous reports that Th17 responses are strongly impaired in mice lacking RARα.[57] That T cells with RARα overexpression, which were primed in the presence of IL-4 in vitro, expressed more IL-4 are in line with the finding that RARα enhances IL-4 in naïve, but not differentiated T cells,[58] which explains the heterogeneous data on T-cell differentiation.[21,23] Of note, RARα-expressing T cells enhance $IgA^{+}$ B cells, indirectly showing that TGF-ß was secreted, as it is the essential IgA switching factor for B cells.[59] However, we did not observe more serum IgA or plasmablasts through RARα-induced Tfh cells. This might be explained by the strong induction of CXCR5 by RARα signaling and therefore loss of the $CXCR5^{low}$ Tfh-cell population which is important for the generation of extrafollicular plasmablasts.[60] However, beyond the T-cell-mediated functions of RARα on the isotype-specific effects of RA on B cells, additional functions by other immune cells, for example, dendritic cells or stromal cells cannot be excluded. In this study, we focused on RARα as a major receptor of 9cRA, as RARβ/γ was not significantly expressed in T and B lymphocytes in this model (data not shown). The RXRs, which also bind 9cRA, are central molecules of the nuclear receptor family and serve as binding partners for several different molecules including the vitamin D receptor, liver x receptors, peroxisome proliferator-activated receptors, and glucocorticoid receptors. As these can also regulate lymphocyte differentiation and/or the cell metabolism, targeting RXRs is an interesting task for future research. The 9cRA was applied s.c. and not orally to avoid a bias through alterations in food consumption and resorption. As the oral

bioavailability of 9cRA is high, and also the Ig response was regulated in low doses,[24] we would expect also effects on the isotype switching after oral intake. Whether 9cRA can be used to therapeutically limit type I allergy is not known, but suggested by preclinical data from established type I allergy with 9cRA-mediated induction of specific IgA at the expense of IgE.

In summary, we deciphered the role of RARα on the humoral allergic immune response by the precise examination of B and T cells at the genetic level and identified cell-specific mechanisms. B cells are primed by RARα signaling toward plasmablast differentiation, while T cells are primed toward a Tfh response. The mechanisms shown here support the adjuvant function of vitamin A on the vaccination-induced humoral immune response, in line with WHO recommendations in vitamin A deficiency regions. Moreover, our findings shed light on the complex physiological mechanisms of the allergic humoral immune response of RARα in lymphocytes and suggest targeting RARα or RARα-gene regulation during inflammation as a candidate to address humoral immune responses distinctly to either optimize vaccination strategies or specific immunotherapies for the treatment of allergic diseases.

## ACKNOWLEDGMENTS

This work was funded by the Deutsche Forschungsgemeinschaft (DFG; SFB-TRR130-P19 to MW and GH and P23 to AH). We thank Toralf Kaiser, Jenny Kirsch, and Ana Catalina Teichmüller for flow cytometry technical support, Katrin Lehmann, Imme Sakwa-Waltz, Christin Sophia Kabus, and the team of the animal facility (Deutsches Rheuma-Forschungszentrum Berlin).

## CONFLICTS OF INTEREST

GH received consultation fees from Allergopharma outside of this work and has lectured at educational events sponsored by Biotest and Eli-Lilly. MW received honoraria or consultation fees by ALK-Abelló Arzneimittel GmbH, Mylan Germany GmbH, Leo Pharma GmbH, Sanofi-Aventis Deutschland GmbH, Regeneron Pharmaceuticals, Inc, DBV Technologies S.A, Stallergenes GmbH, HAL Allergie GmbH, Allergopharma GmbH & Co. KG, Bencard Allergie GmbH, Aimmune Therapeutics UK Limited, Actelion Pharmaceuticals Deutschland GmbH, Novartis AG and Biotest AG. Other authors have nothing to disclose.

## ORCID

*Margitta Worm* https://orcid.org/0000-0002-3449-1245
*Guido Heine* https://orcid.org/0000-0003-1467-9862

## REFERENCES

1. Song W, Craft J. T follicular helper cell heterogeneity: time, space, and function. *Immunol Rev*. 2019;288(1):85-96.
2. Varricchi G, Harker J, Borriello F, Marone G, Durham SR, Shamji MH. T follicular helper (Tfh) cells in normal immune responses and in allergic disorders. *Allergy*. 2016;71(8):1086-1094.
3. Hall JA, Grainger JR, Spencer SP, Belkaid Y. The role of retinoic acid in tolerance and immunity. *Immunity*. 2011;35(1):13-22.
4. Ross AC. Vitamin A and retinoic acid in T cell-related immunity. *Am J Clin Nutr*. 2012;96(5):1166S-1172S.
5. Ertesvag A, Naderi S, Blomhoff HK. Regulation of B cell proliferation and differentiation by retinoic acid. *Semin Immunol*. 2009;21(1):36-41.
6. Wiseman EM, Bar-El Dadon S, Reifen R. The vicious cycle of vitamin a deficiency: a review. *Crit Rev Food Sci Nutr*. 2017;57(17):3703-3714.
7. Surman SL, Penkert RR, Jones BG, Sealy RE, Hurwitz JL. Vitamin supplementation at the time of immunization with a cold-adapted influenza virus vaccine corrects poor mucosal antibody responses in mice deficient for vitamins A and D. *Clin Vaccine Immunol*. 2016;23(3):219-227.
8. Sudfeld CR, Navar AM, Halsey NA. Effectiveness of measles vaccination and vitamin A treatment. *Int J Epidemiol*. 2010;39(Suppl 1):i48-i55.
9. Measles vaccines: WHO position paper. *Wkly Epidemiol Rec*. 2009;84(35):349-360.
10. https://www.who.int/vmnis/vitamina/data/database/countries/en/. Accessed 1 June 2020
11. Larange A, Cheroutre H. Retinoic acid and retinoic acid receptors as pleiotropic modulators of the immune system. *Annu Rev Immunol*. 2016;34:369-394.
12. Theodosiou M, Laudet V, Schubert M. From carrot to clinic: an overview of the retinoic acid signaling pathway. *Cell Mol Life Sci*. 2010;67(9):1423-1445.
13. Takeuchi H, Yokota A, Ohoka Y, et al. Efficient induction of CCR9 on T cells requires coactivation of retinoic acid receptors and retinoid X receptors (RXRs): exaggerated T Cell homing to the intestine by RXR activation with organotins. *J Immunol*. 2010;185(9):5289-5299.
14. Hammerschmidt SI, Friedrichsen M, Boelter J, et al. Retinoic acid induces homing of protective T and B cells to the gut after subcutaneous immunization in mice. *J Clin Invest*. 2011;121(8):3051-3061.
15. Brown CC, Esterhazy D, Sarde A, et al. Retinoic acid is essential for Th1 cell lineage stability and prevents transition to a Th17 cell program. *Immunity*. 2015;42(3):499-511.
16. Iwata M, Eshima Y, Kagechika H. Retinoic acids exert direct effects on T cells to suppress Th1 development and enhance Th2 development via retinoic acid receptors. *Int Immunol*. 2003;15(8):1017-1025.
17. Schwartz DM, Farley TK, Richoz N, et al. Retinoic acid receptor alpha represses a Th9 transcriptional and epigenomic program to reduce allergic pathology. *Immunity*. 2019;50(1):106-120.e10.
18. Mucida D, Park Y, Kim G, et al. Reciprocal TH17 and regulatory T cell differentiation mediated by retinoic acid. *Science*. 2007;317(5835):256-260.
19. Mucida D, Pino-Lagos K, Kim G, et al. Retinoic acid can directly promote TGF-beta-mediated Foxp3(+) Treg cell conversion of naive T cells. *Immunity*. 2009;30(4):471-472. Author reply 472-473.
20. Morikawa K, Nonaka M. All-trans-retinoic acid accelerates the differentiation of human B lymphocytes maturing into plasma cells. *Int Immunopharmacol*. 2005;5(13-14):1830-1838.
21. Chen Q, Ross AC. Retinoic acid promotes mouse splenic B cell surface IgG expression and maturation stimulated by CD40 and IL-4. *Cell Immunol*. 2007;249(1):37-45.
22. Chun TY, Carman JA, Hayes CE. Retinoid repletion of vitamin A-deficient mice restores IgG responses. *J Nutr*. 1992;122(5):1062-1069.
23. Mora JR, Iwata M, Eksteen B, et al. Generation of gut-homing IgA-secreting B cells by intestinal dendritic cells. *Science*. 2006;314(5802):1157-1160.
24. Heine G, Hollstein T, Treptow S, Radbruch A, Worm M. 9-cis retinoic acid modulates the type I allergic immune response. *J Allergy Clin Immunol*. 2018;141(2):650-658.e5.

25. Worm M, Krah JM, Manz RA, Henz BM. Retinoic acid inhibits CD40 + interleukin-4-mediated IgE production in vitro. *Blood*. 1998;92(5):1713-1720.
26. Schindler M, Drozdenko G, Kuhl AA, Worm M. Immunomodulation in patients with chronic hand eczema treated with oral alitretinoin. *Int Arch Allergy Immunol*. 2014;165(1):18-26.
27. Shahinian A, Pfeffer K, Lee KP, et al. Differential T cell costimulatory requirements in CD28-deficient mice. *Science*. 1993;261(5121):609-612.
28. Oxenius A, Bachmann MF, Zinkernagel RM, Hengartner H. Virus-specific MHC-class II-restricted TCR-transgenic mice: effects on humoral and cellular immune responses after viral infection. *Eur J Immunol*. 1998;28(1):390-400.
29. Sonoda E, Pewzner-Jung Y, Schwers S, et al. B cell development under the condition of allelic inclusion. *Immunity*. 1997;6(3):225-233.
30. Zou YR, Takeda S, Rajewsky K. Gene targeting in the Ig kappa locus: efficient generation of lambda chain-expressing B cells, independent of gene rearrangements in Ig kappa. *EMBO J*. 1993;12(3):811-820.
31. Niesner U, Albrecht I, Janke M, et al. Autoregulation of Th1-mediated inflammation by twist1. *J Exp Med*. 2008;205(8):1889-1901.
32. Lahmann A, Kuhrau J, Fuhrmann F, et al. Bach2 controls T follicular helper cells by direct repression of Bcl-6. *J Immunol*. 2019;202(8):2229-2239.
33. Perfetto SP, Chattopadhyay PK, Lamoreaux L, et al. Amine reactive dyes: an effective tool to discriminate live and dead cells in polychromatic flow cytometry. *J Immunol Methods*. 2006;313(1-2):199-208.
34. Van Vu D, Beier KC, Pietzke LJ, et al. Local T/B cooperation in inflamed tissues is supported by T follicular helper-like cells. *Nat Commun*. 2016;7:10875.
35. Kim D, Pertea G, Trapnell C, Pimentel H, Kelley R, Salzberg SL. TopHat2: accurate alignment of transcriptomes in the presence of insertions, deletions and gene fusions. *Genome Biol*. 2013;14(4):R36.
36. Langmead B, Salzberg SL. Fast gapped-read alignment with Bowtie 2. *Nat Methods*. 2012;9(4):357-359.
37. Anders S, Pyl PT, Huber W. HTSeq–a Python framework to work with high-throughput sequencing data. *Bioinformatics*. 2015;31(2):166-169.
38. Liao Y, Smyth GK, Shi W. featureCounts: an efficient general purpose program for assigning sequence reads to genomic features. *Bioinformatics*. 2014;30(7):923-930.
39. Love MI, Huber W, Anders S. Moderated estimation of fold change and dispersion for RNA-seq data with DESeq2. *Genome Biol*. 2014;15(12):550.
40. Faul F, Erdfelder E, Lang AG, Buchner A. G*Power 3: a flexible statistical power analysis program for the social, behavioral, and biomedical sciences. *Behav Res Methods*. 2007;39(2):175-191.
41. Hutloff A. T follicular helper-like cells in inflamed non-lymphoid tissues. *Front Immunol*. 2018;9:1707.
42. Weber JP, Fuhrmann F, Feist RK, et al. ICOS maintains the T follicular helper cell phenotype by down-regulating Kruppel-like factor 2. *J Exp Med*. 2015;212(2):217-233.
43. Nurieva RI, Chung Y, Hwang D, et al. Generation of T follicular helper cells is mediated by interleukin-21 but independent of T helper 1, 2, or 17 cell lineages. *Immunity*. 2008;29(1):138-149.
44. Van Vu D, Bauer L, Kroczek RA, Hutloff A. ICOS costimulation differentially affects T cells in secondary lymphoid organs and inflamed tissues. *Am J Respir Cell Mol Biol*. 2018;59(4):437-447.
45. Fazilleau N, Eisenbraun MD, Malherbe L, et al. Lymphoid reservoirs of antigen-specific memory T helper cells. *Nat Immunol*. 2007;8(7):753-761.
46. Ballesteros-Tato A, Leon B, Graf BA, et al. Interleukin-2 inhibits germinal center formation by limiting T follicular helper cell differentiation. *Immunity*. 2012;36(5):847-856.
47. Oestreich KJ, Weinmann AS. Ikaros changes the face of NuRD remodeling. *Nat Immunol*. 2011;13(1):16-18.
48. Nurieva RI, Podd A, Chen Y, et al. STAT5 protein negatively regulates T follicular helper (Tfh) cell generation and function. *J Biol Chem*. 2012;287(14):11234-11239.
49. Johnston RJ, Choi YS, Diamond JA, Yang JA, Crotty S. STAT5 is a potent negative regulator of TFH cell differentiation. *J Exp Med*. 2012;209(2):243-250.
50. Chen Q, Ross AC. Vitamin A and immune function: retinoic acid modulates population dynamics in antigen receptor and CD38-stimulated splenic B cells. *Proc Natl Acad Sci U S A*. 2005;102(40):14142-14149.
51. Scheffel F, Heine G, Henz BM, Worm M. Retinoic acid inhibits CD40 plus IL-4 mediated IgE production through alterations of sCD23, sCD54 and IL-6 production. *Inflamm Res*. 2005;54(3):113-118.
52. Indrevaer RL, Moskaug JO, Paur I, et al. IRF4 is a critical gene in retinoic acid-mediated plasma cell formation and is deregulated in common variable immunodeficiency-derived B cells. *J Immunol*. 2015;195(6):2601-2611.
53. Ertesvag A, Aasheim HC, Naderi S, Blomhoff HK. Vitamin A potentiates CpG-mediated memory B-cell proliferation and differentiation: involvement of early activation of p38MAPK. *Blood*. 2007;109(9):3865-3872.
54. Pantazi E, Marks E, Stolarczyk E, Lycke N, Noelle RJ, Elgueta R. Cutting edge: retinoic acid signaling in B cells is essential for oral immunization and microflora composition. *J Immunol*. 2015;195(4):1368-1371.
55. Ohoka Y, Yokota A, Takeuchi H, Maeda N, Iwata M. Retinoic acid-induced CCR9 expression requires transient TCR stimulation and cooperativity between NFATc2 and the retinoic acid receptor/retinoid X receptor complex. *J Immunol*. 2011;186(2):733-744.
56. Wang J, Yen A. A novel retinoic acid-responsive element regulates retinoic acid-induced BLR1 expression. *Mol Cell Biol*. 2004;24(6):2423-2443.
57. Hall JA, Cannons JL, Grainger JR, et al. Essential role for retinoic acid in the promotion of CD4(+) T cell effector responses via retinoic acid receptor alpha. *Immunity*. 2011;34(3):435-447.
58. Hoag KA, Nashold FE, Goverman J, Hayes CE. Retinoic acid enhances the T helper 2 cell development that is essential for robust antibody responses through its action on antigen-presenting cells. *J Nutrs* 2002;132(12):3736-3739.
59. Cazac BB, Roes J. TGF-beta receptor controls B cell responsiveness and induction of IgA in vivo. *Immunity*. 2000;13(4):443-451.
60. Odegard JM, Marks BR, DiPlacido LD, et al. ICOS-dependent extrafollicular helper T cells elicit IgG production via IL-21 in systemic autoimmunity. *J Exp Med*. 2008;205(12):2873-2886.


## SUPPORTING INFORMATION

Additional supporting information may be found online in the Supporting Information section.

**How to cite this article:** Scholz J, Kuhrau J, Heinrich F, et al. Vitamin A controls the allergic response through T follicular helper cell as well as plasmablast differentiation. *Allergy*. 2020;00:1–14. https://doi.org/10.1111/all.14581

**Supplementary Table I**: Antibodies used for flow cytometry

| Antibodies for surface staining | | | | Antibodies for intracellular staining | | | |
|---|---|---|---|---|---|---|---|
| **Specificity** | **clone** | **fluorochrome** | **Supplier** | **Specificity** | **clone** | **fluorochrome** | **Supplier** |
| CD4 | RM4-5 | BV 711 | Biolegend | Bcl-6 | K112-91 | A 647 | BD Biosciences |
| CD8a | 53-6.72 | BV 711, BV 785 | eBioscience | Gata-3 | TWAJ | PE-Cy7 | eBioscience |
| CD19 | 6D5 | BV 785 | Biolegend | T-bet | eBio4B10 | BV 605 | eBioscience |
| CD25 | PC 61 | BV 650 | Biolegend | RORγ(t) | AFKJS-9 | PE | eBioscience |
| CD38 | 90 | APC-Cy7, PacB | Biolegend | IgM | Bet-2 | FITC | Own conjugate |
| CD45.1 | A20 | PE-Cy7, PerCP | Biolegend | IgG1 | RMG1-1 | PE-Dazzle | BD Biosciences |
| CD45.2 | 104 | A700 | Biolegend | IgA | C10-3 | PE | BD Biosciences |
| CD69 | H1.2F3 | FITC, PE | BioLegend | IgE | R35-72 | FITC, BV 650 | BD Biosciences |
| CD90.1 | Ox-7 | PerCP, A 700 | Own conjugate | IL-4 | BVD6-24G2 | PE-Cy7 | eBioscience |
| CD138 | 281-2 | Biotin, PacB | BD Biosciences | IL-5 | TRFK5 | A 647 | own conjugate |
| GL7 | GL7 | A 647 | Own conjugate | IL-13 | 38213.11 | PE | own conjugate |
| IL-7R | A7R34 | PE-Dazzle | Own conjugate | IL-17A | TC11-18H10.1 | A 700 | BioLegend |
| CXCR4 | L276F12 | PE | BioLegend | IL-21 | IL-21R-Fc | A 647 | R&D Systems |
| CXCR5 | L138D7 | Biotin | BioLegend | IFN-γ | XMG1.2 | FITC | own conjugate |
| PD-1 | J43 | PE | eBioscience | | | | |
| ICOS | MIC-2043 | A 647 | own conjugate | | | | |

Abbr.: A, Alexa Fluor; BV, Brilliant Violet; Cy7, Cyanin 7; PacB, Pacific Blue; PE, Phycoerythrin; PerCP, Peridinin-Chlorophyll-Protein

# Supplementary Information

## Vitamin A controls the allergic response through T follicular helper cell as well as plasmablast differentiation

Josephine Scholz, Julia Kuhrau, Frederik Heinrich, Gitta Anne Heinz, Andreas Hutloff, Margitta Worm and Guido Heine

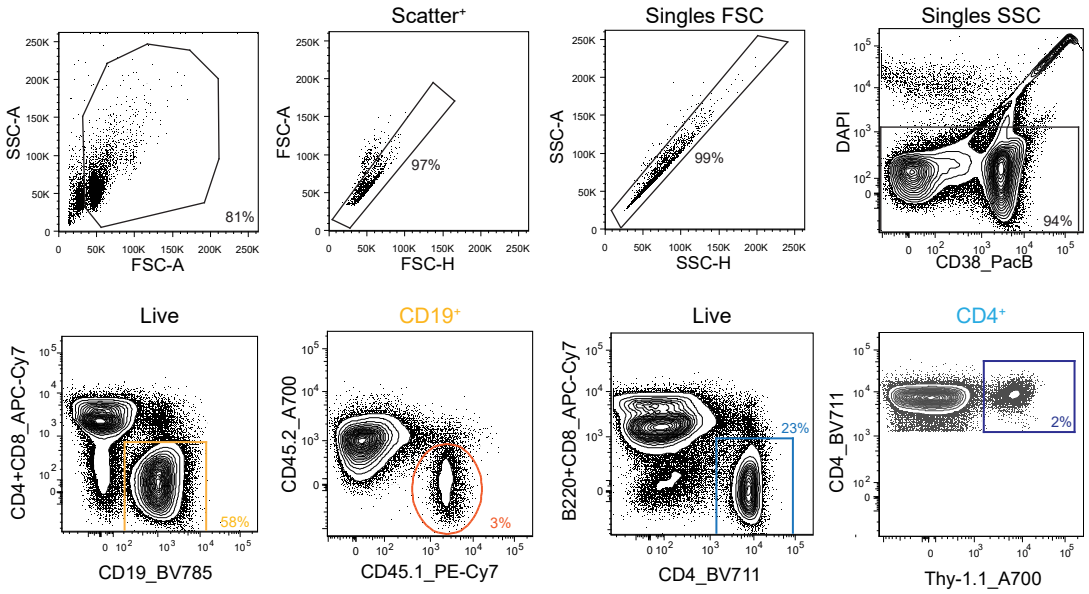


**Supplementary Figure 1.** Flow cytometric gating strategy to identify antigen-specific T and B cells in lung and lymph nodes.

Lymphocytes were identified according to size (forward scatter; FSC-A) and granularity (side scatter; SSC-A). Doublets and dead cells (DAPI$^+$) were excluded afterwards. To identify transgenic B1-8i B cells, gates were set on CD4$^-$ CD8$^-$ CD19$^+$ CD45.2$^-$ CD45.1$^+$ cells. The identification of transgenic Smarta T cells was done by gating on B220$^-$ CD8$^-$ CD4$^+$ Thy-1.1$^+$ cells.

pMSCV-RARα-IRES-mAmetrine

pQCXIX-GFP-U6-shRNA-RARα

**Supplementary Figure 2.** Maps of retroviral vectors.

For constitutive retroviral overexpression, RARα cDNA was cloned into a pMSCV-based vector, which had been modified by insertion of the violet laser-excitable yellow-fluorescing protein mAmetrine after an internal ribosomal entry site (IRES). For specific RNA-interference of RARα, RARα target sequences were designed and cloned into the retroviral vector pQCXIX, containing the U6 promoter driven shRNA expression cassette inserted into the 3' LTR and an EF1α-promotor driven GFP fluorescent reporter.

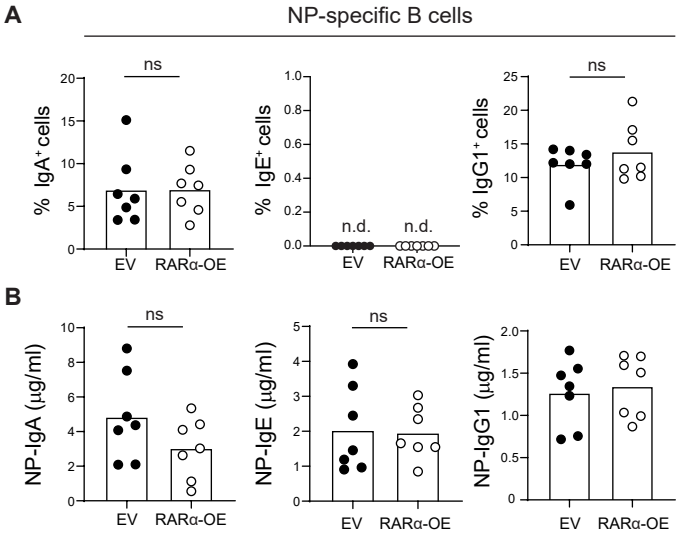


**Supplementary Figure 3.** RARα does not alter class switching directly in B cells.

B cells were analyzed from the airway inflammation model as shown in Figure 2. **(A)** Bar graphs showing the frequency of IgA, IgE, and IgG1 secreting B cells (intracellular staining IgA, IgE, and IgG1) within NP-specific B cells. **(B)** Serum concentrations of antigen-specific IgA, IgE, and IgG1, as determined by ELISA. Each symbol represents a single animal and bars depict the mean. Data are representative of two independent experiments with 4 or 5 animals per group and per experiment. Two-tailed student's t test for normally distributed data or Mann-Whitney test for nonparametric data (Shapiro-Wilk normality test): ns $P > 0.05$.

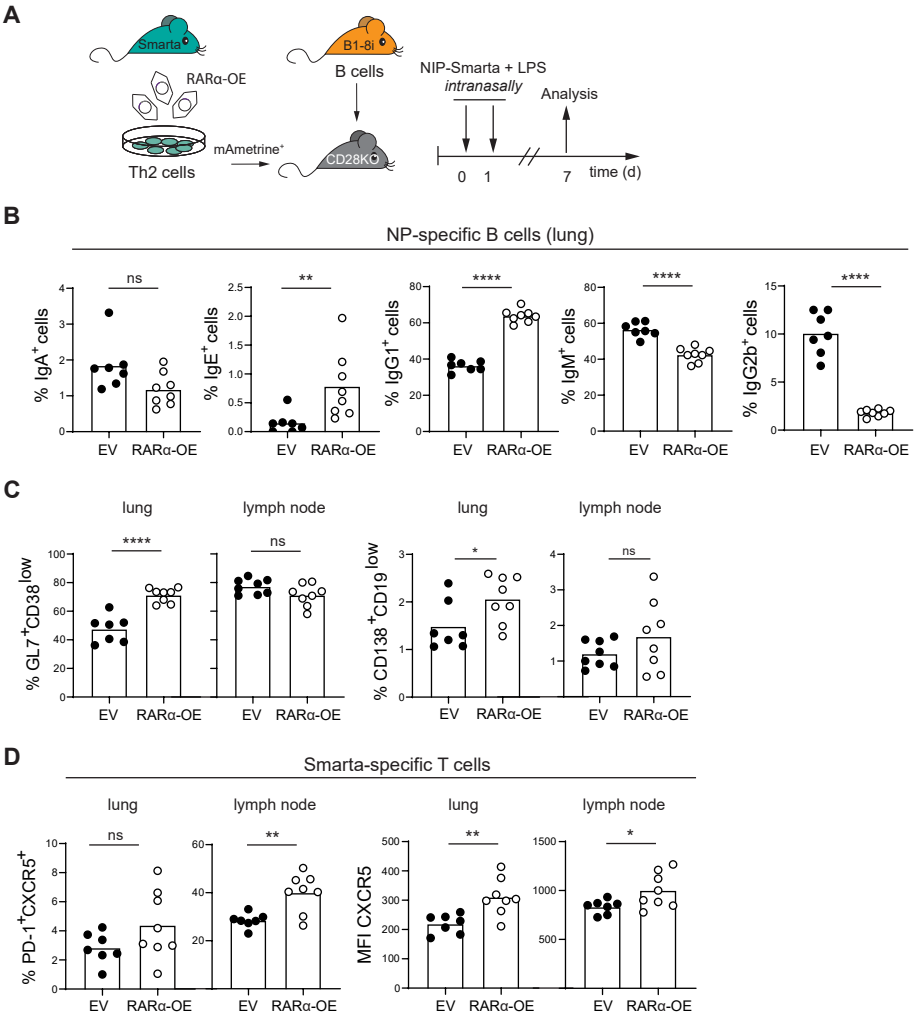


**Supplementary Figure 4.** RARα overexpression promotes Tfh cell and B cell differentiation already after 7 days.

**(A)** Experimental setup for airway inflammation model. Smarta Th2 cells retrovirally transduced with a RARα overexpression vector or empty vector control were adoptively transferred into CD28 KO recipients. On indicated days, mice were immunized with an NIP-Smarta conjugate and LPS intranasally. Antigen-specific B and T cells from lung and lung-draining lymph node were analyzed on day 7. **(B)** Representative flow cytometric staining of NP-specific B cells in the lung regarding the isotype class and bar graphs showing the frequency of IgA, IgE, IgG1, and IgM secreting B cells (intracellular flow cytometric staining for IgA, IgE, IgG1, IgM and IgG2b) within Ag-specific B cells. **(C)** Quantification of $CD38^{low}GL7^{+}$ GC–like B cells in lung tissue and $CD38^{low}GL7^{+}$ GC B cells in lung-draining lymph node and analysis of NP-specific $CD138^{+}CD19^{low}$ plasma cells respectively. Frequencies are shown as percentage of the NP-specific B cells. **(D)** Statistical analysis of $PD\text{-}1^{+}CXCR5^{+}$ Tfh-like cells from lung tissue and $PD\text{-}1^{+}CXCR5^{+}$ Tfh cells from lung-draining lymph node. Frequencies are shown as percentage of the Smarta-specific T cells. Data consists of one experiment with 7 or 8 animals per group. Two-tailed student's t test for normally distributed data or Mann-Whitney test for nonparametric data (Shapiro-Wilk normality test): * $P < 0.05$; ** $P < 0.01$; **** $P < 0.0001$; ns $P > 0.05$.

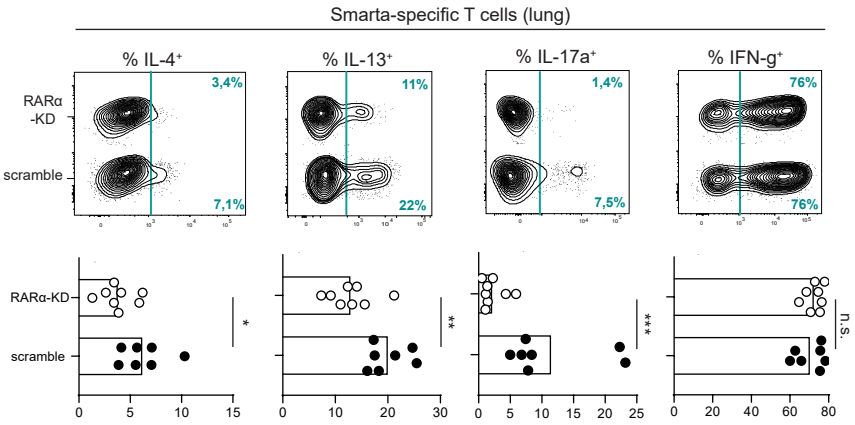


**Supplementary Figure 5.** RARα knockdown in T cells alters their cytokine profile.

Activated Smarta Th2 cells were retrovirally transduced with an shRNA vector for RARα knockdown (RARα-KD) or a scramble sequence and adoptively transferred into recipients. On indicated days, mice were immunized with a NIP-Smarta conjugate and LPS intranasally. Antigen-specific T cells from lung were analyzed on day 17. Data show cytokine expression by antigen-specific T cells. Cells isolated from lung were restimulated *in vitro* with PMA/ionomycin and cytokine expression was analyzed by flow cytometric intracellular cytokine staining. Dots represent individual mice and bars indicate the mean. Data consists of one experiment with 7 or 8 animals per group. Two-tailed student's t test for normally distributed data or Mann-Whitney test for nonparametric data (Shapiro-Wilk normality test): * $P < 0.05$; ** $P < 0.01$; *** $P < 0.001$; ns $P > 0.05$.

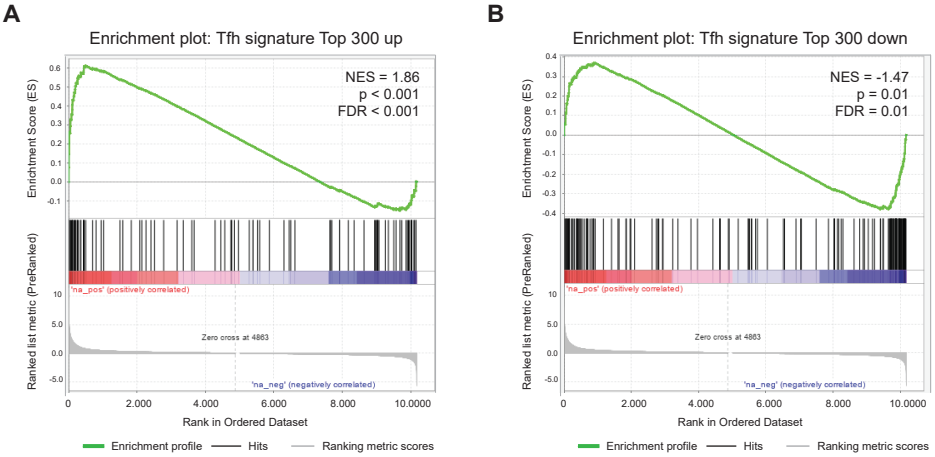


**Supplementary Figure 6.** GSEA reveals a Tfh signature in RARα-overexpressing T cells.

Gene Set Enrichment Analysis of differentially regulated genes showing gene sets upregulated **(A)** or downregulated **(B)** in Tfh cells relative to genes regulated by RARα-overexpressing T cells.